Available online at www.sciencedirect.com

SCIENCE DIRECT®

Magnetic Resonance Imaging 23 (2005) 167–173

MAGNETIC RESONANCE IMAGING

Nuclear magnetic resonance and spin relaxation in biological systems☆

Robert G. Bryant[a,*], Jean-Pierre Korb[b]

[a]Chemistry Department, University of Virginia, PO Box 400319, Charlottesville, VA 22904-4319, USA
[b]Laboratoire de Physique de la Matière Condensée, CNRS UMR 7643, Ecole Polytechnique, 91128 Palaiseau, France

Abstract

Proton nuclear spin-lattice relaxation in biological systems is generally distinguished from that in inorganic systems such as rocks by the presence of locally disordered macromolecular environments. Rapid exchange of readily observed labile small molecules among differently oriented macromolecular sites generally nearly averages the spectral anisotropies in the small molecule resonances. The biological tissue is generally distinguished from the inorganic matrix by the presence of a significant population of protons in the solid components that are well connected by dipolar spin couplings. Magnetic coupling between the solid and the liquid components generally dominates the magnetic field dependence of the spin-lattice relaxation rates observed in the small molecule components which is generally described by a power law in the Larmor frequency. Recent theory involving a modification of the spin-phonon class of relaxation mechanism provides a quantitative understanding of these data in terms of the dynamics of the chain molecules generally present in the solid spin systems, folded proteins for example.

Keywords: Magnetic relaxation dispersion; Spin-lattice relaxation; Spin-phonon coupling; Cross-relaxation; Magnetic coupling

1. Magnetic features of boilogical systems

If we divide materials into biological and nonbiological porous systems, nuclear magnetic resonance and spin relaxation in biological systems have both important similarities as well as important differences from other microporous materials. Like inorganic systems such as zeolites, clays, rocks and porous glasses, the biological systems may present a variety of locally ordered environments that provide dynamic constraints on the trajectories of mobile molecules. The biological systems are generally composed of a relatively extensive but soft matrix of molecules that are solid in the sense that they do not rotate freely, but are soft in that there may be considerable range of internal motion possible, and the biological systems are usually deformable on a macroscopic scale. The inorganic matrix on the other hand is often macroscopically porous, but the matrix is sufficiently cross-linked that the structural support provided to the mobile and readily observed entrapped molecules is rigid and not deformable. An important feature for relaxation is that the natural inorganic systems are often contaminated by considerable paramagnetic ion impurities as both surface bound ions and matrix substitutions in the rigid support. Paramagnetic centers are, of course, present in biological systems as well, but are often well sequestered by macromolecules as in the metalloproteins. Freely diffusing inorganic ions such as iron(II), iron(III) or manganese(II) are rare and do not often contribute to the predominate relaxation pathways except in special circumstances such as blood. Both classes of system may provide considerable short range and sometimes long range organization to observed molecules that may affect the spin relaxation by changing the effective dimensionality of the space sampled by the dynamics of the observed spins. The effects of such local order may change the magnetic field dependence of the spin-lattice relaxation rate dramatically.

An often crucial distinction between inorganic and biological systems is that the inorganic system is often proton-poor; that is, the solid matrix is composed of structures that do not include a well-connected proton spin network. In this case the proton spin relaxation of the observed liquid component, and the magnetic field dependence in particular, may reflect the character of the constrained diffusive processes that drive relaxation. In the majority of biological systems the confining structures are proton-rich; the protons then form a major population of

☆ This work was supported by the National Institutes of Health, USA, the University of Virginia, the Ecole Polytecnhique, and the CNRS, France.
* Corresponding author. Tel.: +1 434 924 1494.
E-mail address: rgb4g@virginia.edu (R.G. Bryant).

0730-725X/$ – see front matter © 2005 Elsevier Inc. All rights reserved.
doi:10.1016/j.mri.2004.11.026

strongly coupled spins that may interact with readily observed spins mobile with which they are in intimate contact. The presence of the large, but generally unobserved solid proton population in a biological sample such as a tissue may have dominant effects on the proton spin relaxation of the observed species including the solvent and a variety of small molecules that may be of metabolic or therapeutic interest. We focus in this discussion on the biological systems and several features of the spin-lattice relaxation processes.

2. Anisotropy

A distinguishing feature of NMR in immobilized systems is that all anisotropies in the system may appear; that is, the chemical shift anisotropy, nuclear electric quadrupole couplings and dipolar couplings are not averaged by rapid rotational motions. One might expect that the spectroscopy of biological systems would then be dominated by the richness of such anisotropic interactions; however, this is usually not the case if low-molecular-weight components are observed. Although biological systems may be locally ordered, it is rare that the systems are uniformly oriented at the molecular level. Fig. 1 represents a cartoon of biological solids that are compositionally identical, but where the local order is different. Both systems are solid and no rotational averaging is observed in the solid components, direct observation of which would reveal the usual solid-state powder pattern spectra showing the usual dipolar, quadrupolar or chemical shift anisotropies. More generally one observes the small molecules because of dramatically increased sensitivity and possibly resolution. In this case, the spectrum, even of a quadrupolar nucleus such as ^{35}Cl or ^{2}H, does not reveal directly the anisotropy of the semisolid system even when the observed spin may reside on a molecule that may bind and exchange with unique binding sites on the solid matrix of molecules. Generally, a broadened Lorentzian line is detected with a narrow central portion and a broader than normal spectral wings as shown in Fig. 1A. This spectrum is essentially rotationally averaged by chemical exchange of the observed small molecule between locally ordered binding sites of different orientation in the magnetic field. In a cross-linked protein, for example, the exchanging spin may sample several hundred sites in the time of a spectral acquisition time, which nearly averages the anisotropy of the sites sampled. Each bound site corresponds to a particular line or pair of lines in the powder pattern, but the next site corresponds to a position in the powder pattern; when several hundred such sites are sampled by each observed molecule, the spectrum collapses as in other rapid chemical exchange cases. However, the solid effects may persist in some ways because the anisotropic interactions are not completely averaged by the exchange processes. Thus, spins such as ^{35}Cl or ^{23}Na ion may often pass multiple quantum filters that a species that never samples a bound anisotropic site does not [1–10].

A distinctly different spectrum results when the local environment is uniformly oriented in the magnetic field as in a crystal, which is shown schematically in Fig. 1B. In this case, exchange of the observed and labile species with these sites averages the spectrum of the isotropic phase with that of the ordered solid phase to an average position. When different locally ordered domains are summed as in a polycrystalline sample, then the result is a powder pattern

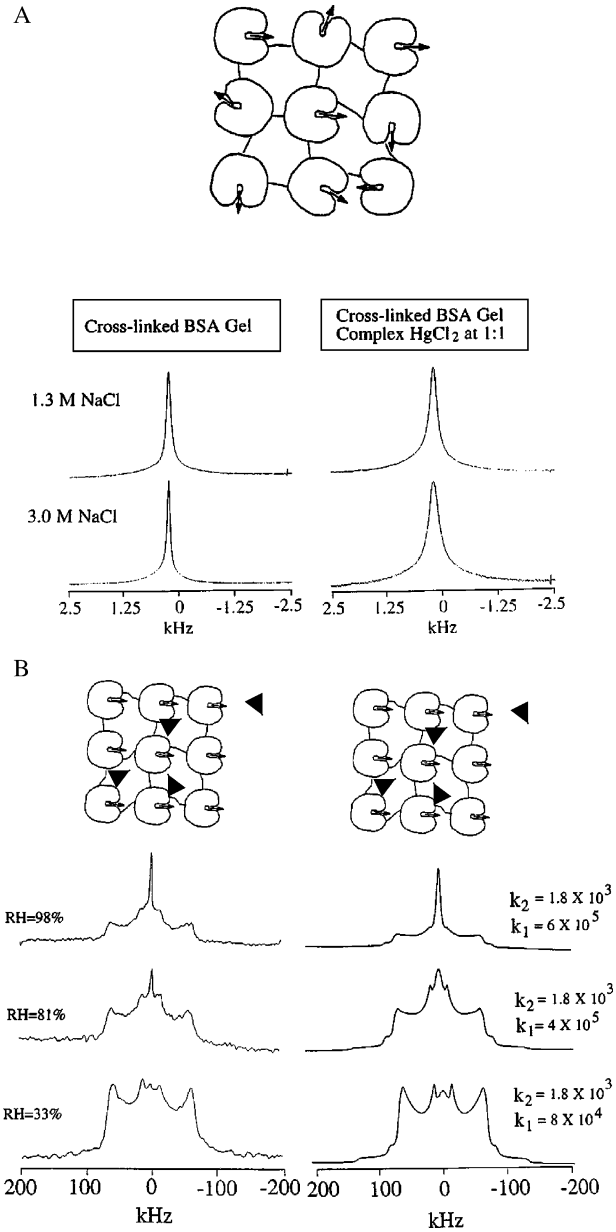

Fig. 1. (A) The ^{35}Cl NMR spectrum of cross-linked serum albumin containing mercury(II) at sulfhydryl sites that provide a strongly bound though rare site for exchange of chloride ion. The detected NMR spectrum in the bulk chloride ion resonance is a super Lorentzian line where the effects of the anisotropy of the bound environment are lost. (B) The ^{2}H NMR spectrum of a phenyl propionic acid in cross-linked crystals of the carboxypeptidase A; the exchange of the phenyl propionic acid with the uniformly oriented binding sites preserves the line shape of the solid environment even though the ligand reorients uniformly in the unbound phase [12].

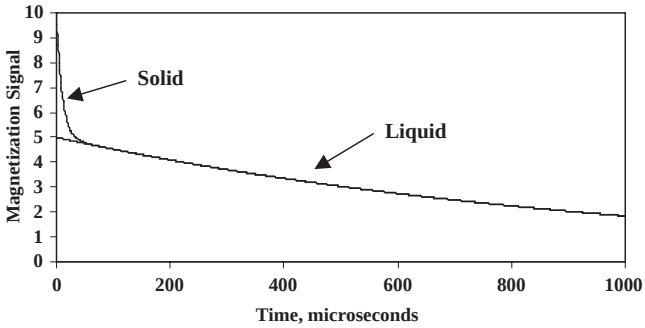

Fig. 2. A computed representative free induction decay of magnetization in a dynamically heterogeneous system such as a tissue containing both solid and liquid components with drastically different values for the transverse relaxation rate.

where the width is scaled by the ratio of the concentration of the bound anisotropic population to that unbound and isotropic phase. In the case shown, the deuterium in an inhibitor exchanges with the active site of carboxypeptidase A in a cross-linked crystal and the spectrum is a scaled powder pattern from which the usual deuterium line shape analysis may be extracted [11,12]. Biological tissues usually do not provide the high degree of local order found in a crystal and spectra like that shown in Fig. 1A are observed. However, important and useful exceptions occur in highly ordered systems where intramolecular dipolar couplings are preserved in the water resonances [7].

3. Relaxation coupling

Although usually not observed in MRI measurements, both the solid and liquid components of biological systems may be detected as shown in Fig. 2. In the time domain, the solid components appear only in the earliest part of the free induction decay often with transverse relaxation time constants in the range of tens of microseconds. It is useful to note that the frequency domain presentation of the same data presents a major dynamic range problem in that the line width of the solid component is usually more than a thousand times wider that that of the liquid or small molecule components; thus, its amplitude at the maximum is approximately a thousand times smaller that that of the liquid even if the two spins are present at the same concentration. Thus, the solid is generally not observed in the Fourier transformed spectrum when the liquid components are displayed and the problem may be seriously aggravated if the spectrometer has a dead time the order of or longer than the short T_2 of the solid signal. The simultaneous detection of liquid and solid components has important practical applications; an example is application to the solid fat index in the food industry [13,14].

In most dynamically heterogeneous biological systems such as tissues, a consequence of the solid components is that the nuclear spin relaxation rate constants of the small molecule spins are affected by magnetic coupling to the solid spins. This spin coupling is often a dominant factor in the proton spin-lattice relaxation. A simple demonstration of the coupling is that following a selective pulse, the magnetization of one population pumps that in the second until the magnetizations equilibrate, then they relax together with a composite rate constant that is given by the roots of the coupled differential relaxation equations as shown in Fig. 3 [15,16]. Thus, it is not appropriate to measure longitudinal magnetization relaxation in a tissue and call the apparent decay constant a T_1 value appropriate to the small molecule measured, water for example, and apply simple relaxation equations to interpret such values.

An interesting application of the coupled relaxation is indirect detection of the solid component spectrum, which is generally tens of kHz wide. Because the spin populations are coupled, perturbation of one population affects the other. A simple implementation is to irradiate the solid component with a preparation pulse that is at a frequency different from the dominant solvent resonance and then detect the amplitude of the solvent proton resonances as a function of the preparation pulse irradiation frequency. An example is shown in Fig. 4 where the effects on three solvent components are detected simultaneously, water, acetone and dimethyl sulfide in a cross-linked serum albumin gel that models tissue approximately. The detailed shape of the resulting solid component spectrum is a function of the strength of the irradiating preparation pulse and the line shape is susceptible to broadening by saturation effects as in continuous wave spectroscopy [17]; however, it is clear in Fig. 4 that the protons of all three solvent components suffer a cross-relaxation with the immobile protein protons. The efficiency of the coupling is different as shown by the different amplitudes in the cross-relaxation spectrum, which is most strongly related to the number of

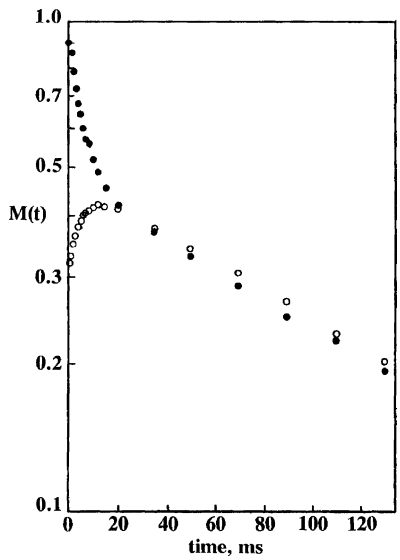

Fig. 3. The response of water and protein proton populations as a function of time following a selective excitation of the water spins. At long times, the two populations decay at identical rates as predicted [64].

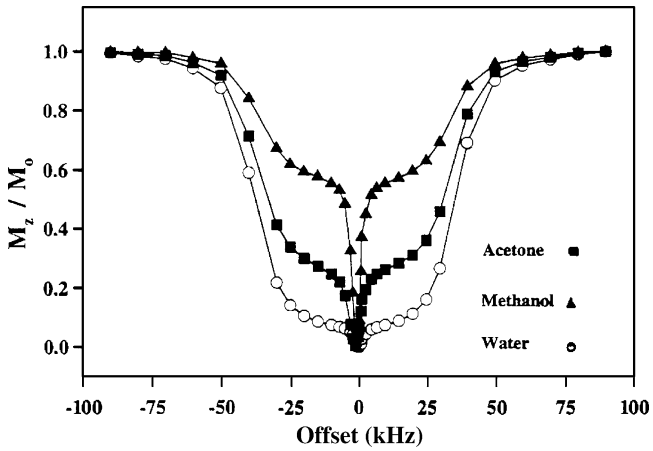

Fig. 4. The proton NMR spectrum of the protein detected by off-resonance irradiation of the protein protons in a cross-linked protein gel containing three solvents: acetone, dimethyl sulfide, and water. The effects of relaxation coupling are apparent in all three solvent resonances [19].

binding sites for the small molecules on the protein [18,19]. The effects of such coupling are general and depend on the dipole–dipole interactions, which have been discussed in detail [20–23]. We point out only that these relaxation coupling effects will be present in the spectra of most proton-containing molecules observed in vivo spectroscopic or imaging experiments.

The magnetic coupling may affect dramatically the magnetic field dependence of the spin-lattice relaxation rates as shown in Fig. 5 where residual water protons are observed in D_2O suspensions of phosphatidyl choline large unilamellar vesicles. By itself, the relaxation rates of the water protons are independent of the magnetic field strength because all of the motions that modulate magnetic couplings are at frequencies much higher than the frequencies utilized in the experiments of Fig. 5. The magnetic field dependence results from a weak coupling between the water protons and the lipid protons [24–33] which transfers the lipid proton dispersion profile to the water protons. Thus, the water proton system may be utilized to characterize the molecular dynamics of the lipid system, which may be described by several complex dynamical models appropriate to chain molecules [34–38].

4. Comprehensive relaxation model

The magnetic field dependence of the water proton spin-lattice relaxation in tissues as well as simpler rotationally immobilized protein systems is described by a power law in the Larmor frequency [39–46] with the exponent typically between 0.5 and 0.8. For a protein solution, the MRD is a Lorentzian dispersion where the inflection point reports the rotational correlation time for the protein reorientating by rotational Brownian motion [47–50]. If the protein rotational motions are stopped by chemical cross-linking at essentially constant composition [39,51], the MRD profile changes from the Lorentzian to a power law as shown in Fig. 6 [39,51]. In both cases, the water proton spin-lattice relaxation rate constant is determined by coupling to the protein protons. The efficiency of the coupling is dominated by exchange of whole water molecules with specific sites on or in the protein where cross-relaxation with the protein protons is efficient. In the solid, the coupling in the bound state is particularly efficient because the bound water molecule is essentially a solid and the cross-relaxation rate

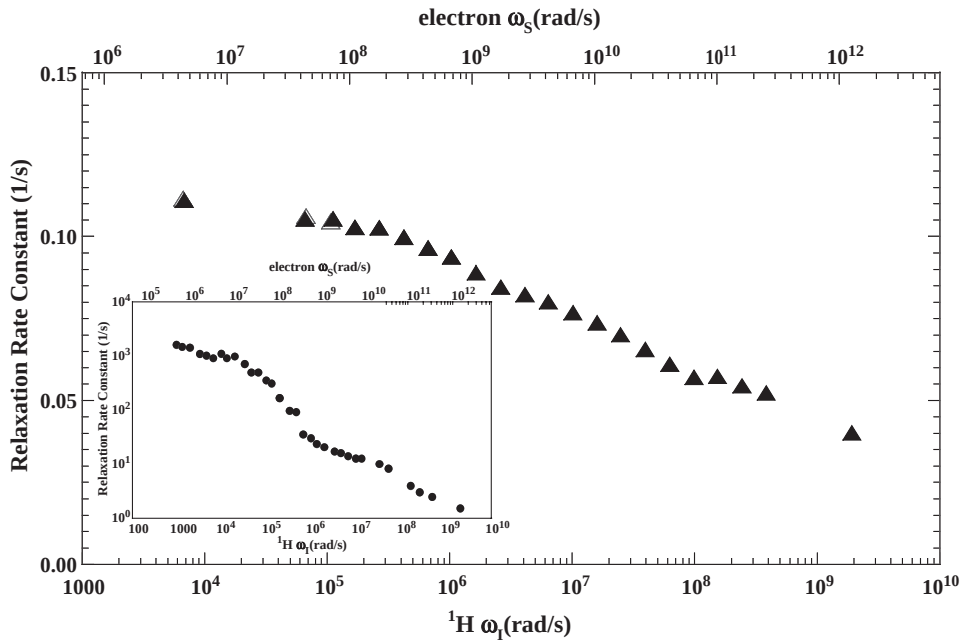

Fig. 5. The magnetic relaxation dispersion profile for residual water protons in D_2O suspensions of large unimellar phosphatidyl choline vesicles at 40 mM and 296 K (K. Victor, R.G. Bryant, unpublished data). The inset is based on data reported by Rommel et al. [66].

constant is essentially the T_2 of the solid proton system or approximately 10 μs. In addition, proton exchange from a variety of labile proton positions on the protein may contribute to the total coupling. Although the tissue represents a complex superposition of contributions, the observed power law is the same and the total spin relaxation of the water protons responds to changes in the concentration of water as predicted by a quantitative treatment of the cross-relaxation coupling [39,51].

Although it has been known for some time that the water proton spins report the magnetic field dependence of the solid component protons, which are described by a power law, the physical origin of the power law has been only recently understood. Kimmich et al. measured the MRD of polypeptides and made the important observation that the power law was present in samples of polyglycine, which has no side chain protons; thus, they suggested that the power law derived from motions of the polypeptide backbone [52]. This idea has recently been put on quantitative foundation by detailed consideration of relaxation induced by spin-phonon coupling [53–56].

The spin-phonon coupling in a three-dimensional crystal is very inefficient relaxation pathway as pointed out by Abragam [57]. However, there is a profound difference between a phonon in a three-dimensional crystal where the correlation of the local disturbance may be lost rapidly and a chain molecule in which the local disturbance may move in an effective space of dramatically reduced dimensionality provided by the chain molecule. In the folded protein, the strong connectivity is in the covalent connectivity provided by the chemical bonds of the polypeptide chain. Although the amino acid side chains are in van der Waals contact in many cases, these connections are weak so that the structural disturbance propagates primarily along the polypeptide chain. The effect of the reduced dimensionality is to increase the efficiency of the spin-phonon coupling by many orders of magnitude [53]. The detailed theory, presented elsewhere [54], provides a quantitative description of the spin-lattice relaxation rate of the protein components of a

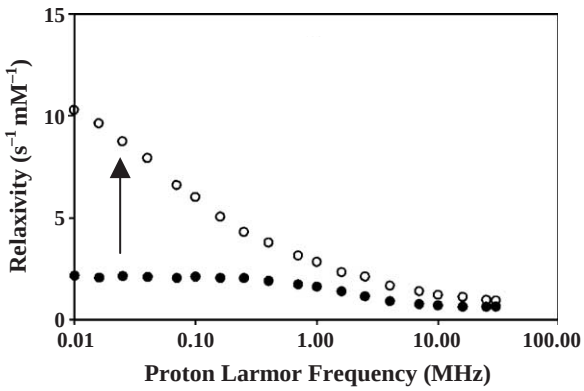

Fig. 6. The water proton magnetic relaxation dispersion profile in 1.8 mM aqueous bovine serum albumin solution and the cross-linked serum albumin gel obtained at the same at the same composition at 298 K [39].

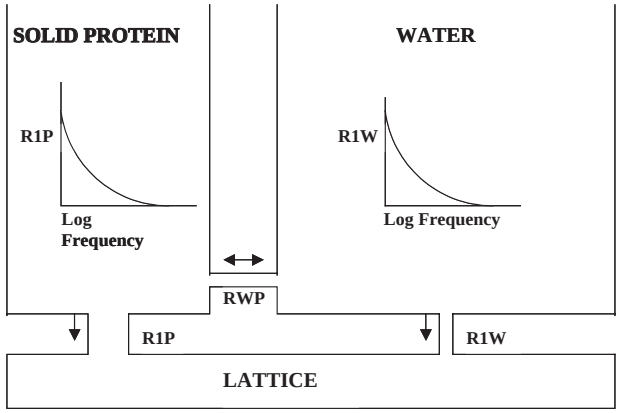

Fig. 7. Schematic representation of relaxation pathways for proton spin relaxation in heterogeneous protein systems that are models for tissues.

protein–water system when the protein is not free to rotate and the effects of the relaxation coupling are included in the complete model. This model accounts for the magnetic field and composition dependence of water and protein proton spin-lattice relaxation rate constants and provides a foundation for understanding the more complex tissue. The essence of the model is summarized in Fig. 7.

The protein proton spin-lattice relaxation is dominated by the structural fluctuations that propagate along the polypeptide chain and which modulate proton–proton dipole–dipole couplings. Motion anywhere relaxes the whole protein proton population because the protons in the rotationally immobilized protein are well coupled to each other, that is, spin diffusion within the protein system is rapid and the population may be said to achieve a common spin temperature in a short time, on the order of T_2 or 10 μs. The water protons are coupled to the protein protons by several magnetic exchange mechanisms, the dominant one being the exchange of whole water molecules with rare binding sites on the protein. The measured field dependence may be discussed in terms of three regions. (1) The region above approximately 10 MHz is dominated by high-frequency motions in the system such as water molecule rotation or methyl group rotation [58–64]. (2) The intermediate field region is dominated by the chain dynamics in the folded protein and displays the characteristic power law in the Larmor frequency. (3) The low field region may present a plateau that in turn may have two causes. (a) Limitations in the magnetization transfer rate between the protein and the water may provide a limitation on the low field rate constant for the water protons. (b) The local magnetic field sensed by protein protons is limited by the effective local dipolar field, which is approximately 11 kHz. Thus, although the applied dc magnetic field that is applied to the sample may be lower than 11 kHz, the effective field dependence of the spin-lattice relaxation rate is truncated by the dipolar field [65]. In summary, in the intermediate field regime, the water proton spin-lattice relaxation is tied to the structural fluctuations in the protein

which propagate primarily along the primary structure of the polypeptide chain.

References

[1] Knubovets T, Shinar H, Eliav U, Navon G. A ^{23}Na multiple-quantum-filtered NMR study of the effect of the cytoskeleton conformation on the anisotropic motion of sodium ions in red blood cells. J Magn Reson B 1996;110(1):16–25.

[2] Assaf Y, Navon G, Cohen Y. In vivo observation of anisotropic motion of brain water using ^{2}H double quantum filtered NMR spectroscopy. Magn Reson Med 1997;37(2):197–203.

[3] Tsoref L, Shinar H, Seo Y, Eliav U, Navon G. Proton double-quantum filtered MRI—a new method for imaging ordered tissues. Magn Reson Med 1998;40(5):720–6.

[4] Eliav U, Navon G. A study of dipolar interactions and dynamic processes of water molecules in tendon by ^{1}H and ^{2}H homonuclear and heteronuclear multiple-quantum-filtered NMR spectroscopy. J Magn Reson 1999;137(2):295–310.

[5] Aletras AH, Tsoref L, Navon G. In vivo ^{1}H double quantum filtered MRI of the human wrist and ankle. Magn Reson Med 2000;43(5):640–4.

[6] Neufeld A, Eliav U, Navon G. New MRI method with contrast based on the macromolecular characteristics of tissues. Magn Reson Med 2003;50(2):229–34.

[7] Navon G, Shinar H, Eliav U, Seo Y. Multiquantum filters and order in tissues. NMR Biomed 2001;14(2):112–32.

[8] Liu D, Knauf PA, Kennedy SD. Detection of Cl^- binding to band 3 by double-quantum-filtered ^{35}Cl nuclear magnetic resonance. Biophys J 1996;70(2):715–22.

[9] Liu D, Kennedy SD, Knauf PA. ^{35}Cl nuclear magnetic resonance line broadening shows that eosin-5-maleimide does not block the external anion access channel of band 3. Biophys J 1995;69(2):399–408.

[10] Bahar S, Gunter CT, Wu C, Kennedy SD, Knauf PA. Persistence of external chloride and dids binding after chemical modification of glu-681 in human band 3. Am J Physiol 1999;277(4 Pt 1):C791–9.

[11] Zhang H, Bryant RG. Characterization of enzyme-bound ligand dynamics by solid-state NMR in the presence of ligand exchange: L-phenylalanine on carboxypeptidase A. Biophys J 1995;68(1):303–11.

[12] Zhang H, Bryant RG. Nuclear magnetic resonance spectra for $I>1$ spins in dynamically heterogeneous systems with chemical exchange among environments. Biophys J 1995;68(6):2556–65.

[13] Lebotlan D, Heliefourel I. Assessment of the intermediate phase in milk-fat by low-resolution nuclear-magnetic-resonance. Anal Chim Acta 1995;311(2):217–23.

[14] Davenel A, Marchal P. Rapid moisture and fat determination by pulsed NMR for monitoring drying and coating processes of extrudates. Int J Food Sci Technol 1995;30(5):655–62.

[15] Edzes HT, Samulski ET. Cross relaxation and spin diffusion in the proton NMR of hydrated collagen. Nature 1977;265:521–3.

[16] Shirley WM, Bryant RG. Proton-nuclear spin relaxation and molecular dynamics in the lysozyme–water system. J Am Chem Soc 1982;104:2910–8.

[17] Grad J, Bryant RG. Nuclear magnetic cross-relaxation spectroscopy. J Magn Reson 1990;90:1–8.

[18] Hinton DP, Bryant RG. ^{1}H magnetic cross-relaxation between multiple solvent components and rotationally immobilized protein. Magn Reson Med 1996;35(4):497–505.

[19] Hinton DP, Bryant RG. Measurement of protein preferential solvation by z-spectroscopy. J Phys Chem 1994;98(33):7939–41.

[20] Bryant RG. Magnetization transfer and cross relaxation in tissue. In: Grant EDM, Harris RK, editors. Encyclopedia of magnetic resonance. New York: Wiley; 1996. p. 2954–62.

[21] Wolff SD, Balaban RS. Magnetization transfer contrast (MTC) and tissue water proton relaxatioin in vivo. Magn Reson Med 1989;10:135–44.

[22] Henkelman RM, Huang X, Xiang QS, Stanisz GJ, Swanson SD, Bronskill MJ. Quantitative interpretation of magnetization transfer. Magn Reson Med 1993;29(6):759–66.

[23] Morrison C, Henkelman RM. A model for magnetization transfer in tissues. Magn Reson Med 1995;33(4):475–82.

[24] Xu ZC, Cafiso DS. Phospholipid packing and conformation in small vesicles revealed by two- dimensional 1h nuclear magnetic resonance cross-relaxation spectroscopy. Biophys J 1986;49(3):779–83.

[25] Ellena JF, Dominey RN, Archer SJ, Xu ZC, Cafiso DS. Localization of hydrophobic ions in phospholipid bilayers using 1h nuclear overhauser effect spectroscopy. Biochemistry 1987;26(14):4584–92.

[26] Holte LL, Gawrisch K. Determining ethanol distribution in phospholipid multilayers with mas-noesy spectra. Biochemistry 1997;36(15):4669–74.

[27] Feller SE, Brown CA, Nizza DT, Gawrisch K. Nuclear overhauser enhancement spectroscopy cross-relaxation rates and ethanol distribution across membranes. Biophys J 2002;82(3):1396–404.

[28] Gaede HC, Gawrisch K. Lateral diffusion rates of lipid, water, and a hydrophobic drug in a multilamellar liposome. Biophys J 2003;85(3):1734–40.

[29] Balaban RS, Ceckler TL. Magnetization transfer contrast in magnetic resonance imaging. Magn Reson Q 1992;8(2):116–37.

[30] Wolff SD, Chesnick S, Frank JA, Lim KO, Balaban RS. Magnetization transfer contrast: MR imaging of the knee. Radiology 1991;179(3):623–8.

[31] Wolff SD, Eng J, Balaban RS. Magnetization transfer contrast: Method for improving contrast in gradient-recalled-echo images. [see comment]. Radiology 1991;179(1):133–7.

[32] Scholz TD, Ceckler TL, Balaban RS. Magnetization transfer characterization of hypertensive cardiomyopathy: Significance of tissue water content. Magn Reson Med 1993;29(3):352–7.

[33] Wolff SD, Balaban RS. Magnetization transfer imaging: Practical aspects and clinical applications. Radiology 1994;192(3):593–9.

[34] Denissov A, Kroutieva M, Fatkullin N, Kimmich R. Segment diffusion and nuclear magnetic resonance spin-lattice relaxation of polymer chains confined in tubes: Analytical treatment and Monte Carlo simulation of the crossover from rouse to reptation dynamics. J Chem Phys 2002;116(12):5217–30.

[35] Kimmich R, Fatkullin N, Seitter RO, Gille K. Chain dynamics in entangled polymers: Power laws of the proton and deuteron spin-lattice relaxation dispersions. J Chem Phys 1998;108(5):2173–7.

[36] Peters A, Kimmich R. The heterogeneous solubility of oxygen in aqueous lecithin dispersions and its relation to chain mobility. A NMR relaxation and wide-line study. Biophys Struct Mech 1977;4(1):67–85.

[37] Spohn KH, Kimmich R. Characterization of the mobility of various chemical groups in the purple membrane of *Halobacterium halobium* by ^{13}C, ^{31}P, and ^{2}H solid state NMR. Biochem Biophys Res Commun 1983;114(2):713–20.

[38] Kimmich R, Fatkullin N. Polymer chain dynamics and NMR. Adv Polym Sci 2004;170:1–113.

[39] Bryant RG, Mendelson DA, Lester CC. The magnetic field dependence of proton spin relaxation in tissues. Magn Reson Med 1991;21(1):117–26.

[40] Spiller M, Brown RD, Koenig SH, Wolf GL. Longitudinal proton relaxation rates in rabbit tissues after intravenous injection of free and chelated Mn^{2+}. Magn Reson Med 1988;8(3):293–313.

[41] Winter F, Kimmich R. NMR field-cycling relaxation spectroscopy of bovine serum albumin, muscle tissue, *Micrococcus luteus* and yeast. ^{14}N^{1}H-quadrupole dips. Biochim Biophys Acta 1982;719(2):292–8.

[42] Koenig SH. Molecular basis of magnetic relaxation of water protons of tissue. Acad Radiol 1996;3(7):597–606.

[43] Koenig SH, Spiller M, Brown RDd, Wolf GL. Magnetic field dependence (nmrd profile) of T_1 of rabbit kidney medulla and urine after intravenous injection of Gd(DTPA). Invest Radiol 1986;21(9): 697–704.
[44] Koenig SH, Brown RDd, Goldstein EJ, Burnett KR, Wolf GL. Magnetic field dependence of proton relaxation rates in tissue with added Mn^{2+}: Rabbit liver and kidney. Magn Reson Med 1985;2(2): 159–68.
[45] Koenig SH, Brown RDd, Adams D, Emerson D, Harrison CG. Magnetic field dependence of T_1 of protons in tissue. Invest Radiol 1984;19(2):76–81.
[46] Koenig SH, Brown RDd. Determinants of proton relaxation rates in tissue. Magn Reson Med 1984;1(4):437–49.
[47] Koenig SH, Schillinger WE. Nuclear magnetic relaxation dispersion in protein solutions. II. Transferrin. J Biol Chem 1969;244(23): 6520–6.
[48] Koenig SH, Schillinger WE. Nuclear magnetic relaxation dispersion in protein solutions. I. Apotransferrin. J Biol Chem 1969;244(12): 3283–9.
[49] Hallenga K, Koenig SH. Protein rotational relaxation as studied by solvent ^1H and ^2H magnetic relaxation. Biochemistry 1976;15(19): 4255–64.
[50] Kiihne S, Bryant RG. Protein-bound water molecule counting by resolution of ^1H spin-lattice relaxation mechanisms. Biophys J 2000; 78(4):2163–9.
[51] Lester CC, Bryant RG. Water-proton nuclear magnetic relaxation in heterogeneous systems: Hydrated lysozyme results. Magn Reson Med 1991;22(1):143–53.
[52] Nusser W, Kimmich R. Protein backbone fluctuations and NMR field-cycling relaxation spectroscopy. J Phys Chem 1990;94(15): 5637–9.
[53] Korb JP, Van-Quynh A, Bryant RG. Proton spin relaxation induced by localized spin-dynamical coupling in proteins. Chem Phys Lett 2001; 339(1–2):77–82.
[54] Korb JP, Bryant RG. The physical basis for the magnetic field dependence of proton spin-lattice relaxation rates in proteins. J Chem Phys 2001;115(23):10964–74.
[55] Korb JP, Bryant RG. Magnetic field dependence of proton spin-lattice relaxation times. Magn Reson Med 2002;48(1):21–6.
[56] Korb JP, Bryant RG. Magnetic field dependence of proton spin-lattice relaxation of confined proteins. C R Physique 2004;5:349–57.
[57] Abragam A. The principles of nuclear magnetism, chapt IX, sect 4c. Oxford: The Clarendon Press, Oxford University Press; 1961. p. 599.
[58] Andrew ER, Gaspar RJ, Vennart W. Proton magnetic relaxation in solid poly(L-alanine), poly(L-leucine), poly(L-valine), and polyglycine. Biopolymers 1978;17:1913–25.
[59] Andrew ER, Bryant DJ, Cashell EM. Proton magnetic relaxation of proteins in the solid state: Molecular dynamics of ribonuclease. Chem Phys Lett 1980;69:551–4.
[60] Andrew ER, Bryant DJ, Cashell EM, Meng QA. A proton NMR study of relaxation and dynamics in polycrystalline insulin. FEBS Lett 1981; 126(2):208–10.
[61] Andrew ER, Bryant DJ, Cashell EM, Meng QA. Solid state dynamics of proteins by nuclear magnetic relaxation. Phys Lett 1982;88A:487–90.
[62] Andrew ER, Bone DN, Bryant DJ, Cashell EM, Gaspar R, Meng QA. Proton relaxation studies of dynamics of proteins in the solid state. Pure Appl Chem 1982;54:585–94.
[63] Andrew ER, Bryant DJ, Tizvi TZ. The role of water in the dynamics and proton relaxation of solid proteins. Chem Phys Lett 1983;95: 463–6.
[64] Shirley WM, Bryant RG. Proton nuclear spin relaxation and molecular dynamics in the lysozyme–water system. J Am Chem Soc 1982;104: 2910–8.
[65] Anoarado E, Ferrante GM. Magnetic field compensation for field-cycling NMR relaxometry in the ulf band. Appl Magn Reson 2003; 24(1):85–96.
[66] Rommel E, Noack F, Meier P, Kothe G. Proton spin relaxation dispersion studies of phospholipid membranes. J Phys Chem 1988;92: 2981–7.